ELSEVIER

International Journal of Mass Spectrometry 210/211 (2001) 249–263

International Journal of Mass Spectrometry

www.elsevier.com/locate/ijms

Matrix-assisted laser desorption/ionization of amphiphilic fullerene derivatives

Tracy Brown[a], Nigel L. Clipston[a], Nafeesa Simjee[a], Heinrich Luftmann[b], Hartmut Hungerbühler[c], Thomas Drewello[a,*]

[a]*Department of Chemistry, University of Warwick, Coventry CV4 7AL, England, United Kingdom*
[b]*Organisch-Chemisches Institut, Universität Münster, Correnstrasse 40, D-48149 Münster, Germany*
[c]*Fachbereich Pharma- und Chemietechnik, Technische Fachhochschule Berlin, Luxemburger Strasse 10, D-13353 Berlin, Germany*

Received 11 January 2001; accepted 6 February 2001

Abstract

Matrix-assisted laser desorption/ionization (MALDI) coupled with reflectron time-of-flight mass spectrometry has been applied to the analysis of fullerene derivatives. As a common structural feature, the derivatised fullerenes comprised a long chained, organic ligand connected via a methylene bridge to the [60]fullerene. Using a structurally similar model analyte, this investigation includes the screening of fourteen different compounds regarding their suitability as MALDI matrices. The appearance of positive- and negative-ion mass spectra has been detailed, and the analysis has been supported by post source decay experiments. It was found that the performance of 9-nitroanthracene, which is currently one of the most universally used matrices for the analysis of fullerene derivatives, is exceeded by some of these materials. In the negative-ion mode, excellent performance has been achieved using the two structurally related β-carboline alkaloids, harmane and *nor*-harmane, as matrices. However, the best results for the analytes investigated here have been obtained employing 2-[(2 E)-3-(4-*tert*-butylphenyl)-2-methylprop-2-enylidene]malononitrile (DCTB). This matrix provides analyte signals in both ion modes at comparatively lower threshold laser fluences, leading to mass spectra, which display a very low degree of unwanted dissociations of the analyte. The formation of molecular analyte ions prevails, rather than ionization occurring via protonation or deprotonation. DCTB also efficiently promotes metal ion attachment to suitably ligated fullerene derivatives. (Int J Mass Spectrom 210/211 (2001) 249–263) © 2001 Elsevier Science B.V.

Keywords: Matrix-assisted laser desorption/ionization; Matrix; fullerene derivatives; Mass spectrometry

1. Introduction

The chemistry of tailor-made derivatization of fullerenes has tremendously advanced over the last several years [l,2]. An enormous wealth of synthetic methods has been developed to modify the all-carbon sphere by, for instance, ligand attachment reactions. Though the geometrical features are often aesthetically appealing, more importantly these compounds provide new material properties, which make them attractive in many areas of modern science. In this context, mass spectrometry plays an essential role as an analytical tool, contributing to the progress in this field.

* Corresponding author. E-mail: t.drewello@warwick.ac.uk

Dedicated to Professor Nico Nibbering, on the occasion of his imminent retirement, in appreciation of his seminal contributions to the field of gas-phase ion chemistry.

PII S1387-3806(01)00429-8

Most synthetic approaches towards new fullerene derivatives are unselective, often leading to a large number of ligands attached to the carbon core. Furthermore, isomerism contributes to the diversity of the products formed. As a consequence, a sensitive analysis is required at an early stage of the synthetic route to identify the desired product, which is then to be separated from unwanted by-products. A further complication, as far as the application of "conventional" ionization methods is concerned, is the need to transfer the neutral molecule into the gas phase without inducing dissociation. Most fullerene derivatives are solid and of only low vapor pressure, so that, upon heating, these compounds readily release the ligands to regenerate the fullerene core. In an effort to achieve "soft" evaporation and ionization of derivatized fullerenes, partial success has been achieved applying those ionization methods that avoid a harsh heating of the sample. Improved performance has been reported, for instance, using field desorption, [3] low temperature fast atom bombardment (FAB), [4] FAB involving noncovalent inclusion complexes of the fullerene derivative with cyclodextrin [5,6], and desorption chemical/electron ionization (DCI, DEI) [7,8]. Although the sample evaporation in DCI and DEI is based on heating, the mean path of the evaporated molecules to reach the location at which the ionization occurs is drastically reduced compared to conventional electron ionization or chemical ionization, resulting in less decomposition. Despite the long-standing assumption that fullerenes are "inactive" to the analysis by electrospray ionization (ESI), there has been promising progress to apply ESI [9–11] without the need of earlier reported modifications of the sample solution [12] or derivatization of the fullerene compound [l3]. Recently, it has been even possible to apply nanospray ionization to obtain molecular ions free of fragmentation and requiring only trace amounts of sample material [14].

However, at present matrix-assisted laser desorption/ionization (MALDI) [15] can surely be regarded as one of the most successful methods for the analysis of derivatised fullerenes. The prominent use of MALDI as a means to analyze fullerene-based materials is most evident from the frequent quotations in the synthetic literature. Despite this widespread use of MALDI, very few beneficial investigations detailing the experimental essentials of the MALDI analysis can be found. Besides instrumental parameters, the nature of the matrix compound is undoubtedly one of the most important experimental features influencing the outcome of the MALDI analysis. The variety of different fullerene derivatives makes it rather unlikely that one particular matrix compound is of universal applicability. Hydrogenated fullerenes, for example, have been successfully analyzed using a special matrix combination, whereby the analyte undergoes less fragmentation due to additional cooling by liberation of gas molecules from a comatrix during the desorption process [16]. For the analysis of fluorofullerenes, the use of highly fluorinated matrix compounds has been tested successfully [17]. The present investigation is concerned with the analysis of monoligated, organic fullerene derivatives, which are amphiphilic in nature [18]. Amphiphilic fullerenes have recently attracted interest in Langmuir-Blodgett film formation and as building blocks for macromolecular micells.

2. Experimental

All MALDI experiments have been accomplished by the use of a commercial reflectron time-of-flight mass spectrometer (Kratos Kompact MALDI IV, Kratos Inc., Manchester, United Kingdom). Recent applications of this instrument in fullerene research can be found [19–21]. The sample activation has been achieved applying a nitrogen laser providing ultraviolet light of 337 nm with a pulse width of 3 ns and a pulse frequency of 1.5 Hz. The instrument operates a continuous acceleration voltage of 20 kV. The drift region preceding the reflectron houses a deflection electrode (the ion gate), which allows for the selection of ions as a function of their arrival times at the gate and has been utilized here for post source decay (PSD) experiments [22]. Each individual time-of-flight (TOF) mass spectrum shown represents the accumulation of 200 single-laser-shot spectra. The resolution remained insufficient to resolve the isotopic pattern of the ions in the mass range of interest. For

instance, to distinguish between the ionized, molecular analyte ion and its protonated or deprotonated quasimolecular ion, some experiments have been carried out using a higher resolving, linear TOF instrument (LAZARUS IIIDE, home built, University of Münster), applying delayed extraction.

Using the model analyte (vide infra) the matrix-to-analyte ratio was varied for several of the matrices under investigation with the aim to achieve a reasonable signal-to-noise ratio with optimum analyte ion abundance at a low degree of fragmentation. A molar matrix-to-analyte ratio of 1000:1 was found to fulfill these requirements and was used to record all the MALDI mass spectra discussed in this paper (except for the spectra shown in Fig. 2). The analyte and matrix solutions were freshly prepared for each analysis in the following manner. The analyte has been dissolved in toluene at a ratio of 1 mg analyte per 1 mL solvent, determining the respective concentration for the matrix solutions with which the analyte solutions were mixed before the analysis. Most matrix solutions were prepared using acetone as the solvent. To achieve better solubility, methanol was used as the solvent for some of the β-carboline matrices, including harmol, harmalol, and harmaline. The molar matrix-to-analyte ratio of 1000:1 was obtained by thoroughly mixing the appropriate volumes of analyte and matrix solutions. The resulting solution was applied from a syringe onto the stainless steel sample slide and dried in an air stream preceding the insertion into the ion source of the mass spectrometer.

3. Results and discussion

The design of the "ideal" matrix compound for the MALDI analysis of a given analyte has as of yet not been achieved. The goal to determine the structural requirements of a matrix to promote the efficient and fragmentation-free desorption and ionization of the analyte, based on its structural peculiarities is hampered by the overall complexity of the desorption/ionization process. As a consequence, the screening of matrices is based to a great extent on trial and error approaches considering compounds that worked successfully as matrices for similar analytes or which underwent certain structural modifications with the intention to improve their matrix performance. In the present investigation, 14 different organic compounds have been examined regarding their performance as matrices for the MALDI analysis of methylene bridged, long chain ligand-bearing fullerene derivatives.

The structures of these analytes and the matrix materials are depicted in Fig. 1. The long-chained fullerene derivatives were available here in trace amounts only, so that the actual testing of the various matrices could not be performed using these analytes. A more abundantly available model analyte was chosen, mimicking some of the relevant features of the amphiphilic fullerenes. In a separate investigation into the electron impact behavior of derivatives featuring the same methylene bridging between fullerene and ligand, the bis(isopropyl carbonyl)methylene adduct to C_{60} (also shown in Fig. 1) was found to be much more thermally labile than the corresponding ethyl- and n-propyl-analogue. This thermal lability probably matches some of the potential difficulties that can be anticipated for desorption of the long-chained analytes as intact moieties. Therefore, the isopropyl derivative was chosen as the model analyte for the screening of the matrices.

Regarding the choice of the matrix compounds, 9-nitroanthracene (9-NA) appears to represent the currently most successful "fullerene matrix" [23–27], thus providing the benchmark to which the performance of other potential matrices has to be measured. Six of the matrices were chosen because of their well-established general applicability to the MALDI analysis of a vast variety of compounds. This group of "classic matrices" includes 2,5-dihydroxybenzoic acid (DHB), Sudan Orange G, α-cyano-4-hydroxycinnamic acid (α-CHC), 3,5-dimethoxy-4-hydroxycinnamic acid (sinapinic acid), 5-methoxysalicylic acid (MSA) and 2-(4-hydroxyphenylazo)benzoic acid (HABA). A further group of matrices is formed from six closely related β-carboline alkaloids. These "β-carboline matrices" were recently shown to possess a remarkably broad applicability [28,29]. This group of compounds includes *nor*-harmane, harmane, harmine,

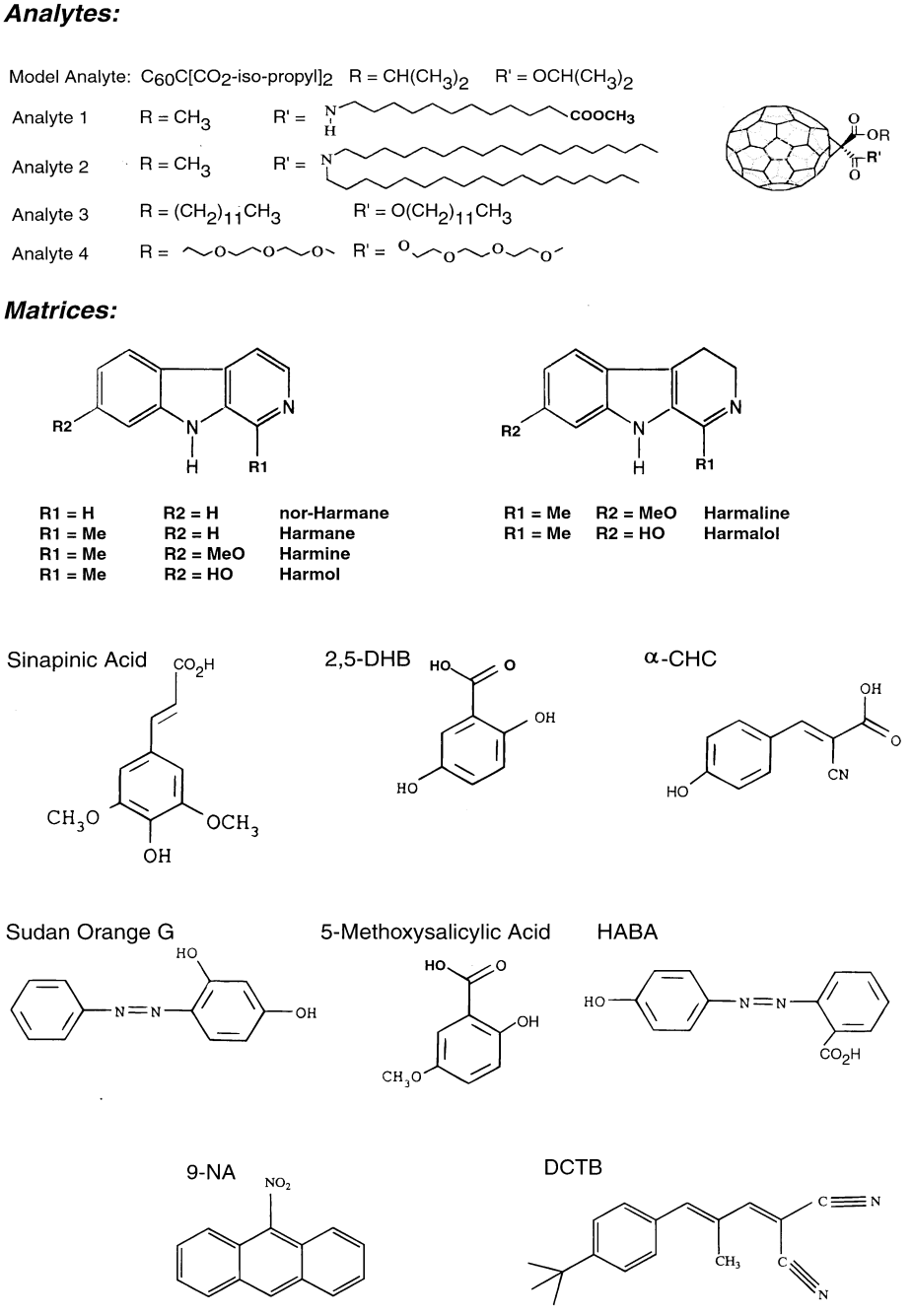

Fig. 1. Structures of the analytes and the matrices investigated in this study.

harmol, harmalol, and harmaline. These matrices were included into this investigation, as the applicability of these compounds has not yet been tested on fullerene analytes. And finally, there is 2-[(2 E)-3-(4-*tert*-butylphenyl)-2-methylprop-2-enylidene] malononitrile (DCTB), a compound that has been success-

fully applied as a MALDI matrix to the analysis of fullerene derivatives [30,31] and which has been only very recently reported to promote the ion formation at considerably reduced threshold laser fluences, leading to very "clean" mass spectra often entirely free of unwanted decomposition of the analyte [32].

The most widely used matrix for the MALDI analysis of fullerene derivatives has clearly been 9-NA [23–27]. Even for the analysis of hydrogenated fullerenes for which a special matrix combination has been successfully applied, whereby the analyte suffers less fragmentation due to additional cooling by liberated gas molecules during the desorption process [16], it has been recently possible to obtain mass spectra of almost the same quality by simply applying 9-NA as matrix [33]. However, in the course of this investigation we find that two major problems can arise in connection with the use of 9-NA as a fullerene matrix.

First, the facile transfer of oxygen from the matrix to the analyte can occur and second, above a certain laser threshold, this matrix shows the tendency to efficiently form larger cluster ions, interfering with the mass region of interest. Both phenomena are evident in the spectra shown in Fig. 2. The negative-ion mass spectrum of $C_{60}C(CO_2CH_2CH_2CH_3)_2$, the n-propyl analogue of the iso-propyl model compound used here for the screening of the matrices, using 9-NA as the matrix. The efficient transfer of up to four oxygen atoms to the analyte is clearly visible, together with the formation of $C_{60}O_n^-$, with n=1 and 2, which are not fragment ions that directly result from analyte dissociations. Additional analysis clearly shows that the degree of oxidation of the neutral sample is far less than what could be suggested from this MALDI spectrum. Especially for the identification of fullerene oxide samples, the uptake of additional oxygen atoms is a most unwanted process [23–27]. A strong indication that the oxides observed are indeed the result of oxygen attachment occurring in the desorption/ionization process provides the laser fluence dependence for the formation of these ions. Above the threshold of ion formation, the abundance of the oxygenated species increases with laser fluence until dissociation eventually prevails. This is in contrast to the desorption/ionization behavior of fullerene oxides as the initial target material, which shows an almost immediate decline in abundance caused by the loss of the oxygen functionality. In Fig. 2(b), a positive-ion mass spectrum is shown using the same analyte and matrix, illustrating the problem connected with the clustering of the matrix. In the present case, cluster ions arising from laser-induced coalescence reactions of the activated matrix are efficiently formed, interfering with the mass range of interest. Although a detailed mass analysis of those clusters is not provided here, their origin from laser ablation of 9-NA is clearly evidenced by the close match to the spectrum shown in Fig. 2(c), which represents the positive-ion mass spectrum of the pure matrix without analyte. The extent to which both these unwanted phenomena are observed clearly depends on the individual case and although 9-NA has been successfully applied as a fullerene matrix, these examples show that there is demand for a more suitable matrix compound.

As illustration to accompany the following discussion, several selected examples of the obtained MALDI mass spectra are depicted in Fig. 3. The positive- and negative-ion MALDI mass spectra of the model analyte are shown using as the respective matrix harmane [Figs. 3(a) and 3(d)], Sudan Orange G [Figs. 3(b) and 3(e)], and MSA [Figs. 3(c) and 3(f)]. There is no analyte ion observed in the positive-ion mode, featuring the pronounced formation of $C_{60}H_x^+$, $C_{61}H_x^+$, and $C_{62}H_x^+$ ions (vide infra for a discussion detailing the assignment of these signals). In the negative-ion mode, a clear trend is revealed, where harmane exhibits the best performance of the three matrix compounds. The base peak in the respective spectrum [Fig. 3(d)] is caused by the intact analyte ion, which is accompanied by a relative low extent of fragmentation.

The performance of the various matrices referring to the MALDI analysis of the model analyte is summarized in Table 1. The table commences with DCTB and 9-NA, followed by the six β-carboline alkaloids and the six classic matrices. For both the positive- and the negative-ion mode, performance criteria were given a grading of 1, 2, and 3, referring to features such as the abundance of the analyte ion, the extent to which fragment ions were observed, and

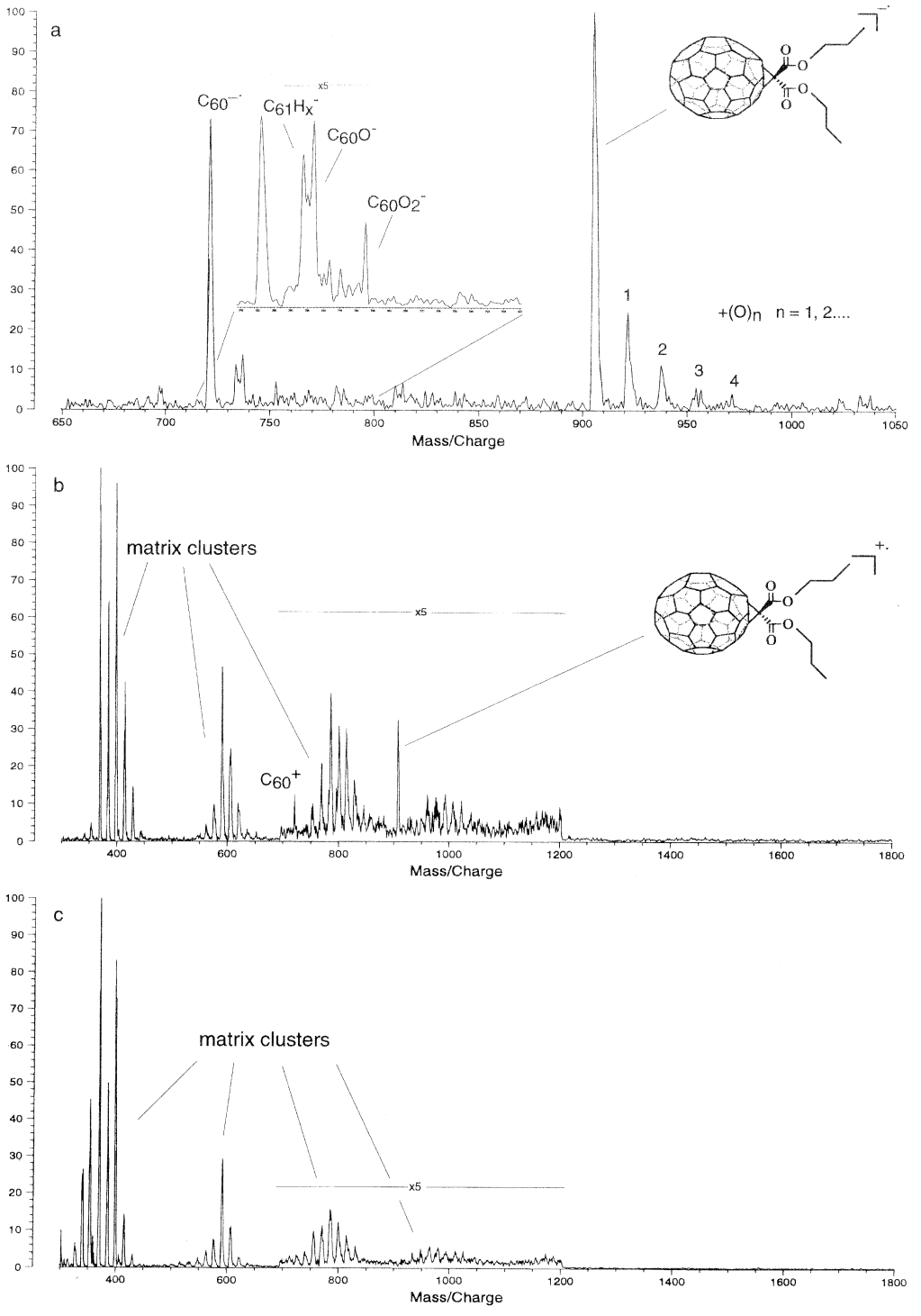

Fig. 2. (a) Partial negative-ion MALDI mass spectrum of $C_{60}C(CO_2CH_2CH_2CH_3)_2$, using 9-NA as the matrix. (b) Partial positive-ion MALDI mass spectrum of $C_{60}C(CO_2CH_2CH_2CH_3)_2$, using 9-NA as the matrix. (c) Partial positive-ion LDI mass spectrum of 9-NA.

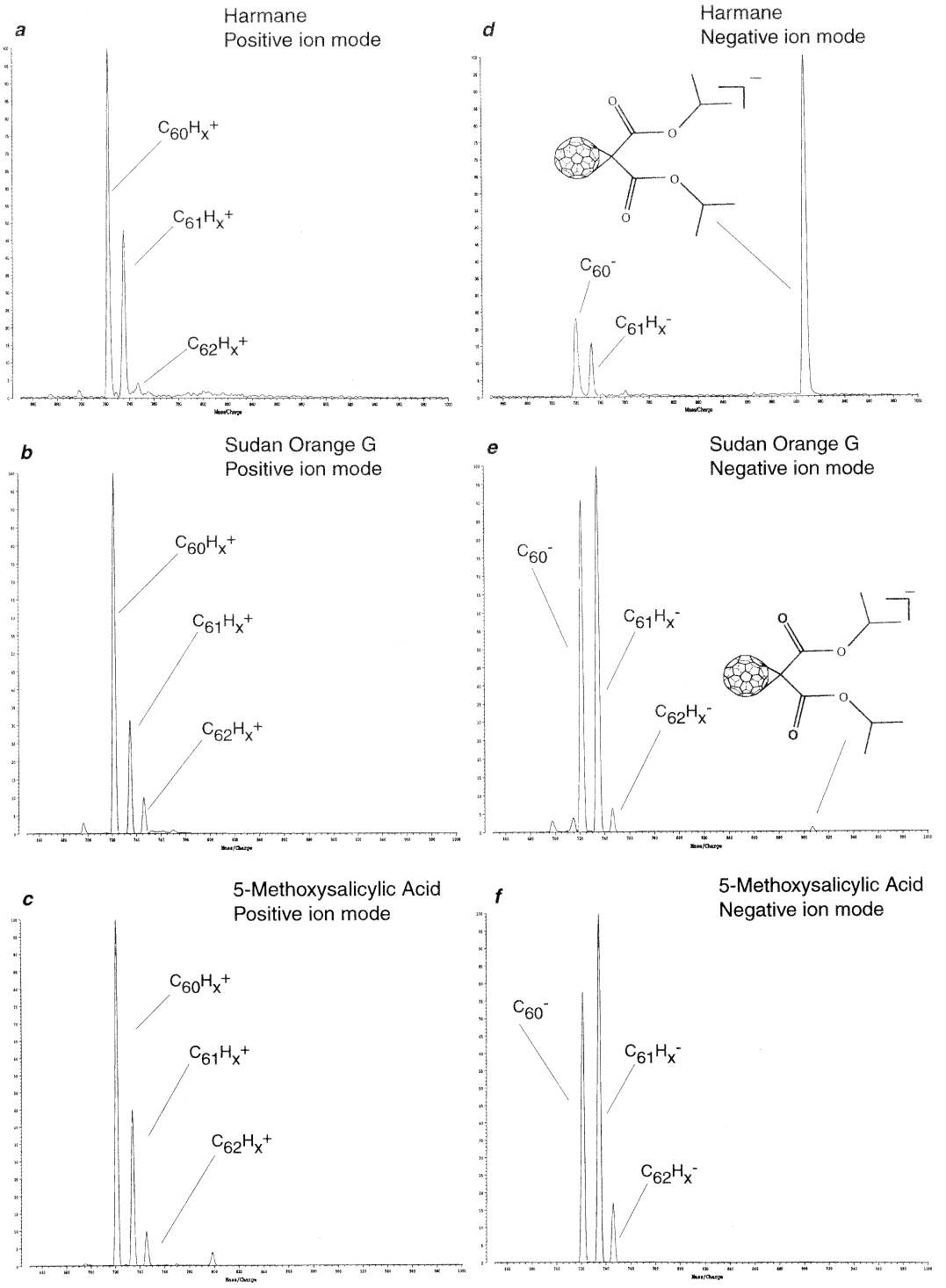

Fig. 3. Partial positive-ion MALDI mass spectra of the model analyte using (a) harmane, (b) Sudan Orange G, and (c) 5-methoxysalicylic acid as the matrices and the corresponding negative-ion results for (d) harmane, (e) Sudan Orange G, and (f) 5-methoxysalicylic acid.

Table 1
Summary of the MALDI performance of the different matrices for the positive and the negative ion mode and using the model analyte

	Positive Ion Mode			Negative Ion Mode		
	Cleanness[a]	Analyte Ion[b]	Fragmentation[c]	Cleanness[a]	Analyte Ion[b]	Fragmentation[c]
DCTB	1	1	2	1	1	1
9 - NA	2	1	2	2	2	2
Norharmane	2	3	2	1	1	2
Harmane	2	3	2	2	1	2
Harmine	2	3	2	2	2	2
Harmol	2	3	2	2	2	2
Harmalol	3	3	2	2	3	2
Harmaline	1	3	1	3	2	2
2,5 - DHB	1	3	2	1	2	2
Sudan Orange G	2	3	2	2	2	2
α - CHC	2	3	3	2	2	3
Sinapinic Acid	1	3	2	2	2	2
5 - Methoxysalicylic Acid	1	3	2	2	3	2
HABA	2	3	3	2	3	2

[a] **Cleanness**; 1 = very clean, 2 = some baseline noise, and 3 = noisy spectra.
[b] **Analyte Ion**; 1 = abundant ion signal, 2 = analyte ion observed, and 3 = analyte ion not observed.
[c] **Fragmentation**; 1 = very little or no fragmentation 2 = some fragmentation observed, and 3 = high level of fragmentation.

the overall cleanness of the spectrum. Depending on the respective criterion, a mark of 1 could represent the formation of an abundant analyte ion, the occurrence of only very minor fragmentation, or a very clean mass spectrum showing only little baseline noise. Increasing marks represent an increasingly unfavorable deviation from the desired appearance of the MALDI spectrum. It is important to note that the general appearance of a particular MALDI mass spectrum can also be strongly influenced by instrumental parameters. This in turn means that the outcome of a particular MALDI experiment can be different for different instrumentation. Statements made here regarding, for example, the extent to which fragmentation is observed or the inability to detect a particular analyte signal, might not be true to the same degree when using different instrumentation. However, the rating of the various compounds in terms of their relative quality in performance as fullerene matrix materials should not depend on the experimental setup.

In the positive-ion mode, most of the matrices gave very poor results indeed. Besides 9-NA and DCTB, the classic matrices and the β-carboline alkaloids failed in the present experiments to produce analyte ions. In contrast, most matrices allowed the detection of the analyte signal in the negative-ion mode. From the classic matrices, DHB and Sudan Orange G were found to be well suited for the use in the negative-ion mode, with an overall performance that matches the one of 9-NA. The spectra obtained using sinapinic acid and α-CHC were of lesser quality, whereas MSA and HABA both failed to produce a detectable analyte ion signal. Regarding the β-carboline alkaloids, harmaline, and harmalol cannot be recommended as suitable matrices, using the latter compound, no analyte signal could be detected. The performance of harmine and harmol almost matched the matrix features of 9-NA. Harmane and even more clearly, *nor*-hamane were found to exceed the performance of the "benchmark matrix", 9-NA. Although a certain degree of fragmentation is still observed, the use of both these matrices leads to more abundant analyte ions and in particular *nor*-harmane provided very clean spectra. As a result, both compounds may be recommended as matrices superior to 9-NA for the analysis of similarly structured fullerene derivatives in the negative-ion mode. By a clear margin, however,

DCTB is found to be the best suited matrix compound for the posed analysis. Not only in the negative-ion mode, but also for the analysis of positive ions, DCTB yielded the most abundant analyte ion signals with an extremely low extent of fragmentation and a remarkable cleanness of the mass spectra resulting in an overall universal applicability, which is not reached by any of the other materials under investigation. The present experiments confirm recent findings by which the use of DCTB reduces dramatically the threshold laser fluences required for the formation of ions in the desorption/ionization process [32]. This in turn might lead to less excitation of the analyte, drastically reducing the occurrence of the unwanted decomposition of the analyte. For this investigation, DCTB had to be synthesized [32]. However, this compound is now also commercially available (Fluka). Summarizing these matrix-screening experiments, DCTB is found as the best-suited matrix for the MALDI analysis of the model analyte and possesses, together with 9-NA, universal applicability in both ion modes. In the negative-ion mode, the use of harmane and *nor*-harmane leads to even better results than MALDI with 9-NA.

Before discussing the MALDI analysis of the long-chained title analytes, the fragmentation behavior of the model analyte is detailed in the following. The positive-ion MALDI mass spectrum [Fig. 4(a)] is contrasted with the respective negative-ion mass spectrum [Fig. 4(b)] and a comparison is made to the corresponding PSD spectra of the isolated cation [Fig. 4(c)] and anion radical [Fig. 4(d)]. In these experiments, 9-NA has been used as the matrix. The accurate mass assignment of the signals observed in the MALDI mass spectra has been accomplished by making use of a higher resolving instrument (see Sec.2), providing isotopically resolved signals (not shown). These experiments clearly reveal that under the applied conditions only the molecular ions of the analyte are formed and that protonation or deprotonation can be discounted as a major path towards the analyte ion formation.

The abundant C_{60} fragment ion is in both ion modes accompanied by ions with a C_{61} carbon content. Although C_{60} is also protonated in the positive-ion mode, the C_{61} fragment shows in both ion modes in addition to the pure carbon cluster also the abundant attainment of at least one additional hydrogen. The same is true for the low abundant C_{62} fragment in both spectra. The $C_{61}H^-$ ion has recently been detected in electrospray experiments with related compounds and structurally analyzed by computational means. [34] It follows that the additional carbon atom is exohedrally attached to C_{60} as a CH entity.

The positive-ion MALDI mass spectrum [Fig. 4(a)] contains three additional signals between those peaks caused by $C_{62}H_x^+$ and the molecular ion. These signals are centered at *m/z* 760, *m/z* 778 and *m/z* 804, and might be tentatively assigned to ions such as $C_{60}CCO^{+\cdot}$(ketene-like), $C_{60}C(H)CO_2H^{+\cdot}$ and $C_{60}C(CO)_2O^{+\cdot}$(anhydride), respectively. The high resolution experiments indicate that the "ketene-like" and the "anhydride" ion are accompanied by their protonated analogues, whereas also ions caused by the loss of hydrogen can be observed below *m/z* 778. The corresponding positive-ion PSD mass spectrum of the molecular ion of $C_{60}C[CO_2CH(CH_3)_2]_2$, shown in Fig. 4(c), features only one daughter ion signal, which is centered at *m/z* 804. Although the PSD experiments could only be performed with low resolving power, thus leading to unresolved peaks, the broad PSD signal centered at *m/z* 804 is entirely attributed to the unimolecular formation of the $C_{60}C(CO)_2O^{+\cdot}$ ion. This assignment is based in analogy on separate dissociation experiments applying a 4-sector tandem mass spectrometer to record the unimolecular daughter ions derived from the molecular ion of the ethyl analogue of the model analyte under high resolution conditions. These experiments clearly indicate the unimolecular formation of $C_{60}C(CO)_2O^{+\cdot}$ daughter ions. The PSD spectrum in Fig. 4(c) was obtained at a laser fluence close to the threshold value for the formation of ions. At higher laser fluences, the spectrum was dominated by signals caused by the delayed electron emission from C_{60} fragments. The influence of ions resulting from delayed ionization on this type of experiment has been detailed elsewhere [19]. The assignment of the corresponding negative ions [Fig.

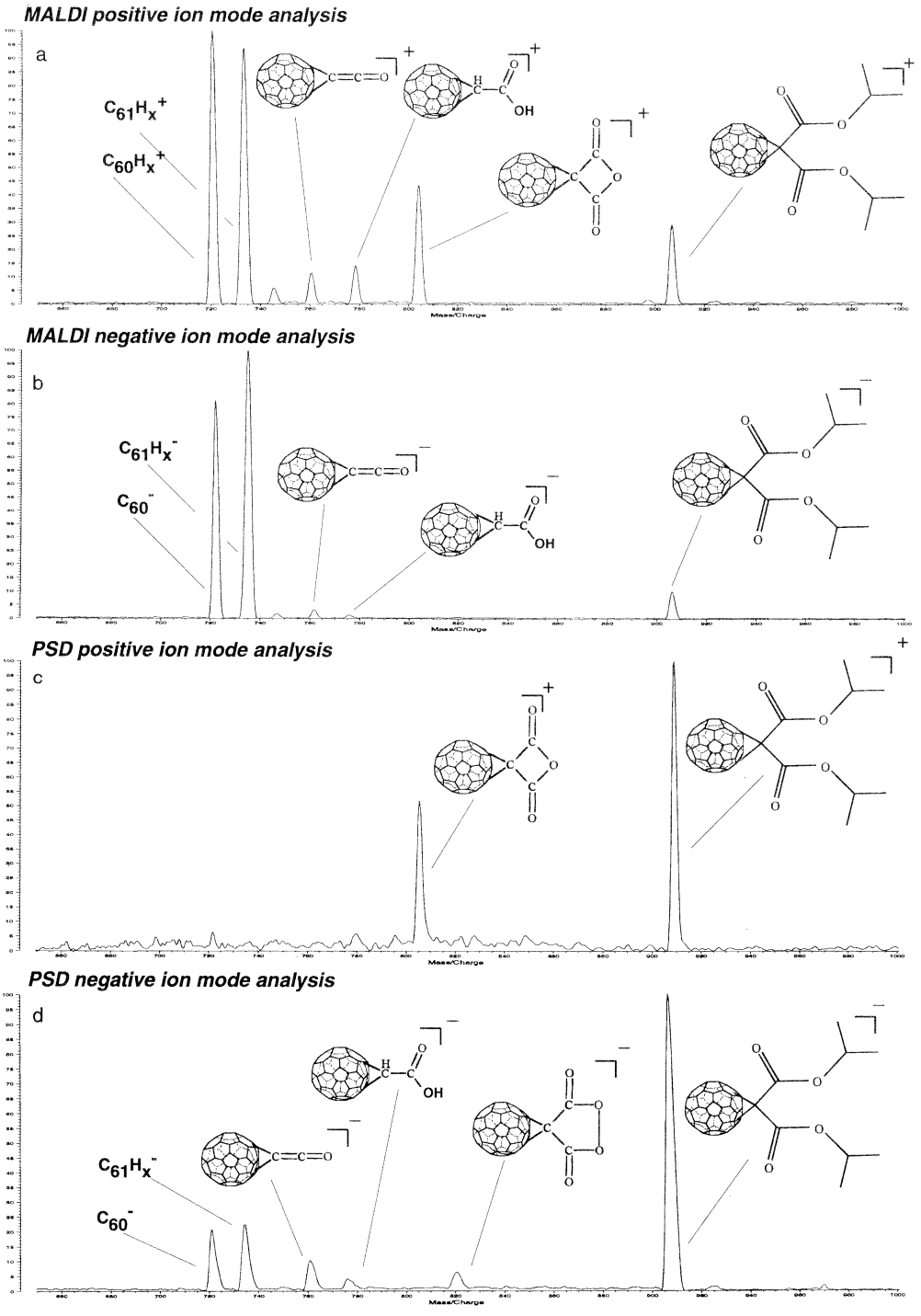

Fig. 4. (a) Partial positive-ion MALDI mass spectrum of the model analyte using 9-NA as the matrix, (b) shows the corresponding partial negative-ion MALDI mass spectrum, (c) positive-ion PSD mass spectrum of the molecular model analyte ion, and (d) the corresponding negative-ion PSD mass spectrum.

4(b)] is complicated by the lower fragment ion abundances in this mass range. For the ketene-like ion, centered at *m/z* 760, similar considerations as those made for the positive ions seem to be valid. The signal previously observed at *m/z* 778 in the positive-ion mode appears to be shifted by one or two mass units to lower masses, owing to the loss or absence of hydrogen in the corresponding ion. Although the anhydride ion is entirely absent, a new fragment ion signal is observed at around *m/z* 820. This signal, which is more pronounced in the corresponding negative-ion PSD spectrum [Fig. 4(d)], might be caused by the loss of both isopropyl moieties from the analyte ion and a plausible structure for it is given in Fig. 4(d). In summary, the MALDI mass spectra are of very similar appearance in both ion modes. The PSD mass spectra, however, reveal that the unimolecular decay involving the attached ligand proceeds for the two charge states via distinct reaction channels.

Guided by the findings derived from the reported screening experiments for suitable matrices, the long-chained fullerene derivatives have been analyzed using *nor*-harmane as the matrix for the negative-ion mode and DCTB for the analysis of the resulting positive ions. The negative-ion MALDI mass spectra of the four different amphiphilic fullerenes 1–4 (see Fig. 1 for structures) are shown in Figs. 5(a)–5(d), respectively. Each of these spectra is governed by only two major signals, consisting of the C_{60}^- fragment ion and the abundantly observed negative molecular ion signal of the respective analyte. The assignment of the analyte signal as being exclusively caused by the molecular ion is in these cases an assumption that is based on the findings derived from the high resolution experiments on the model analyte, as the mass accuracy in these experiments was insufficient to provide unequivocal insight. While analyte 4 displays the lowest tendency to undergo fragmentation, analyte 2 appears to represent the most fragile derivative, which also features the longest chain in the ligand attachment. The spectrum shown as Fig. 5(e) at the bottom results from a MALDI experiment on an equimolar mixture of all five analytes (including the model compound) at the same total analyte-to-matrix ratio as applied throughout. This experiment was conducted to reveal the appearance of the different molecular analyte ions in relation to each other. Although the model analyte provides the most abundant signal by a small margin, its intensity is clearly similar in magnitude compared to the other analytes, confirming that this compound truly represents a most suitable model system for this investigation. Though numerous parameters might influence the absolute analyte ion abundance, the relative intensities of the analyte signals of the samples, seem to reflect their tendency to undergo fragmentation, as discussed for the MALDI analysis of the pure compounds.

The positive-ion MALDI mass spectra of the four title analytes 1–4 are depicted in Figs. 6(a)–6(d), respectively. As in the negative-ion mode, the spectra are comprised only of the C_{60}^+ fragment ion signal (note that a possible contribution from $C_{60}H_x^+$ ions cannot be excluded) and signals caused by intact analyte ions. The most intriguing observation, however, consists in the finding that the molecular ions derived by the analytes 1, 2, and 4 are accompanied by signals that are caused by the attachment of sodium and potassium ions to the neutral analyte. The identity of these signals is undoubtedly confirmed by the mass differences observed between the signals in the analyte ion region. For analyte 2, the sodiated analyte ion signal is dramatically more abundant than the molecular ion signal. The exohedral metal attachment to pure fullerenes has been achieved in earlier gas-phase experiments. Stable complexes could be obtained either in ligand displacement reactions [35] or by direct attachment of the metal ion to the fullerene [36]. In the present case, however, it seems more likely to assume that the metal ion is located on the ligand, rather than attached to the fullerene core. This assumption is supported by the fact that neither the C_{60} fragments, nor the analyte 3 [Fig. 6(c)], studied under essentially the same conditions as the other analytes, show any sign of metal ion attachment. This in turn implies that the nature of the ligand is of decisive importance for the complexation of the metal ion. As all materials were practically free of any alkali metal impurities, the metal ions must have originated

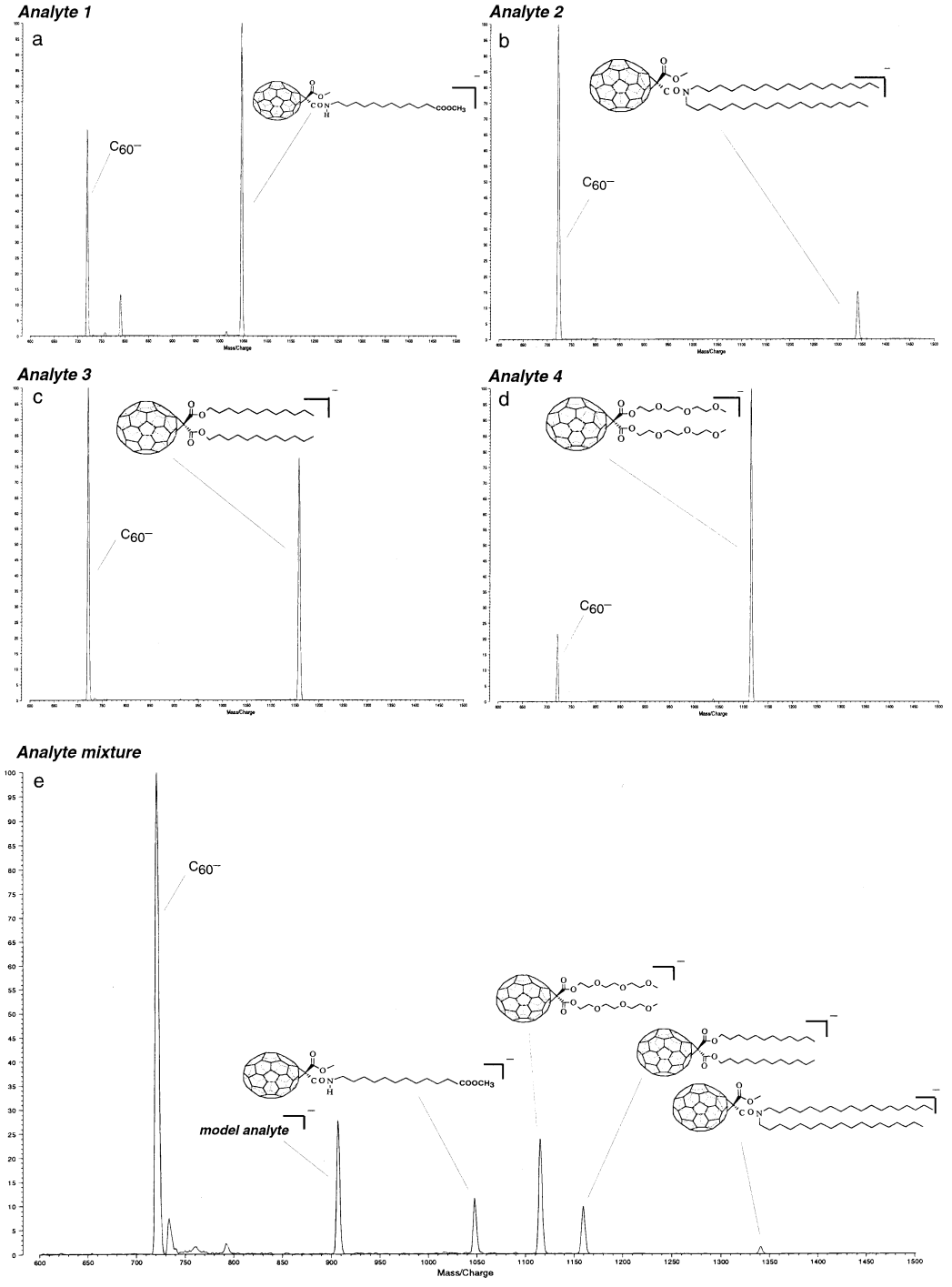

Fig. 5. Partial negative-ion MALDI mass spectra using *nor*-harmane as the matrix for (a) analyte 1, (b) analyte 2, (c) analyte 3, (d) analyte 4, and (e) an equimolar mixture of the analytes 1–4 and the model analyte.

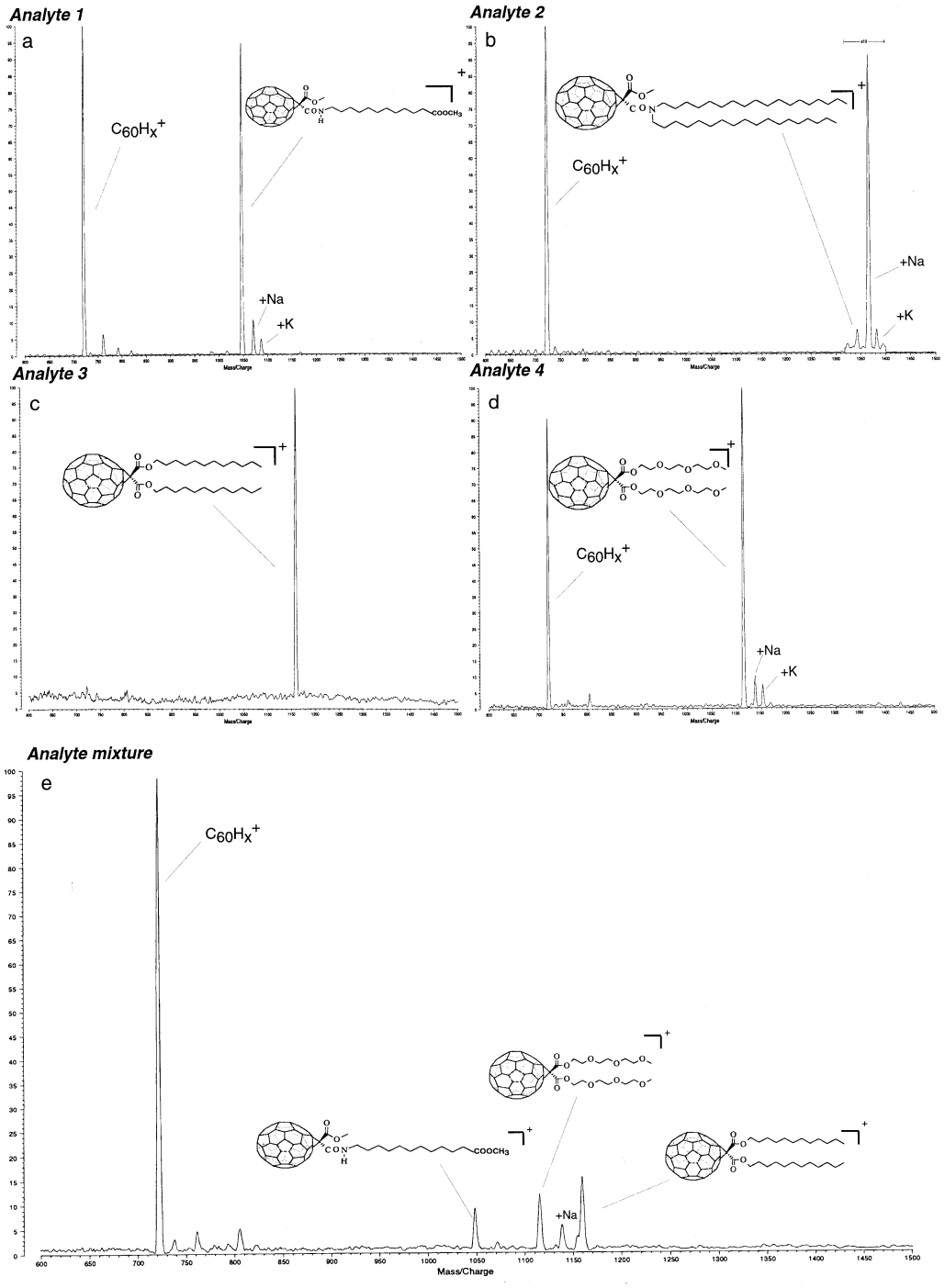

Fig. 6. Partial positive-ion MALDI mass spectra using DCTB as the matrix for (a) analyte 1, (b) analyte 2, (c) analyte 3, (d) analyte 4, and (e) an equimolar mixture of the analytes 1–4.

from the stainless steel target holder. It has to be assumed, that the actual process by which the metal attaches to the analyte has to occur in the gas phase, whereby metal ions liberated from the target surface attach to the desorbing analyte in the fast expanding laser desorption plume. This type of cationization is unprecedented for MALDI of fullerene derivatives and depending on the ligand, has potentially valuable analytical implications. It is interesting to note, that the method of choice to analyze polymers by MALDI represents this very type of analyte cationization, whereby the metal ions are desorbed from a salt layer deliberately added to the analyte/matrix-target [37–39]. Furthermore, the metal ion attachment to a particular type of fullerene derivative has been used in conjunction with electrospray ionization. In these experiments, a crown ether ligand acted as the site for the metal ion complexation [13]. The ion formation mechanism in this approach has not been examined in detail, but it seems likely to assume, that unlike in the present MALDI experiments, the preformation of ions in solution might be of essential importance, which in the electrospray process are liberated into the gas phase following evaporation of the solvent. The ligand of analyte 4 could even be regarded as a ring-opened crown ether (see Fig. 1), which probably represents an attractive complexation site for the metal ion. Although no complexation has been observed for both the model analyte and analyte 3, the efficient metal ion attachment to the analytes 1 and 2 is probably caused by the presence of the nitrogen atom in the ligands, promoting this process.

As in the investigation of the negative-ion spectra, the appearance of the various positive analyte ions as derived from a target containing an analyte mixture has been also examined in the positive-ion mode. The result is shown in Fig. 6(e) for an equimolar mixture of the four title analytes 1–4, retaining the same ratio of the total amount of analytes and the DCTB matrix. As revealed by the MALDI analysis of the individual samples, the analyte 2 shows the greatest tendency to fragment and there is practically no signal found for this analyte using the analyte mixture. The other analytes are detected in comparable abundances.

4. Conclusion

The screening of potentially suitable matrix materials for the MALDI analysis of organic ligand-bearing fullerene derivatives identifies three compounds exceeding the performance of 9-NA, which is known as an appropriate matrix for the fullerene analysis. In the negative-ion mode, the use of two β-carboline alkaloids, harmane, and *nor*-harmane, as matrices leads to cleaner spectra, less fragmentation and more abundant analyte ions than the use of 9-NA. However, a significantly improved performance in both ion modes has been achieved by the use of DCTB as the matrix, which also promoted the analyte ion formation by metal ion attachment. DCTB thus represents the best-suited matrix material for this class of analytes.

Acknowledgements

The authors are pleased to acknowledge the financial support from the EPSRC and The Leverhulme Trust. Professor K.-D. Asmus (Notre Dame) who initiated this collaboration and to Sharon Lau, Richard Jerome, and James Toplis who helped with some of the experiments in the course of their project work at the University of Warwick, are thanked. The authors are indebted to Dr. M.P. Barrow for the critical reading of the manuscript and to Dr. Y.V. Vasil'ev for many helpful comments. Furthermore, Dr. M. Drögemüller (BASF) is acknowledged for providing advice regarding the synthesis of DCTB. Last but not least, T.D. takes great pleasure to thank Nico Nibbering in this way for the unforgettable time spent as a post-doc in his group in 1989/90.

References

[1] A. Hirsch, The Chemistry of the Fullerenes, Thieme, Stuttgart, 1994.
[2] R. Taylor, Lecture Notes on Fullerene Chemistry: A Handbook for Chemists, Imperial College, London, 1999.
[3] C. Rüchardt, M. Gest, J. Ebenhoch, H.-D. Beckhaus, E.E.B.

Campbell, R. Tellgmann, H. Schwarz, T. Weiske, S. Pitter, Angew. Chem. Int. Ed. Engl. 32 (1993) 584.
[4] J.H. Gross, S. Giesa, W. Krätschmer, Rapid Commun. Mass Spectrom. 13 (1999) 815.
[5] C.-G. Jou, L.-L. Shiu, C.K.-F. Shen, T.-Y. Luh, G.-R. Her, Rapid Commun. Mass Spectrom. 9 (1995) 604.
[6] S. Giesa, J.H. Gross, R. Gleiter, W. Krätschmer, Eur. Mass Spectrom. 4 (1998) 189.
[7] L. Dunsch, U. Kirbach, K. Klostermann, J. Mol. Struct. 348 (1995) 381.
[8] A.D. Darwish, A.K. Abdul-Sada, G.J. Langley, H.W. Kroto, R. Taylor, D.R.M. Walton, J. Chem. Soc., Perkin Trans. 2 (1995) 2359.
[9] T.-Y. Liu, L.-L. Shiu, T.-Y. Luh, G.-R. Her, Rapid Commun. Mass Spectrom. 9 (1995) 93.
[10] J.-P. Deng, C.-Y. Mou, C.C. Han, J. Phys. Chem. 99 (1995) 14907.
[11] J.C. Hummelen, B. Knight, J. Pavlovich, R. Gonzalez, F. Wudl, Science 269 (1995) 1554.
[12] K. Hiraoka, I. Kudaka, S. Fujimaki, H. Shinohara, Rapid Commun. Mass Spectrom. 6 (1992) 254.
[13] S.R. Wilson, Y. Wu, J. Chem. Soc., Chem. Commun. (1993) 784.
[14] M.P. Barrow, X. Feng, J.I. Wallace, O.V. Boltalina, R. Taylor, P.J. Derrick, T. Drewello, Chem. Phys. Lett. 330 (2000) 267.
[15] F. Hillenkamp, M. Karas, Int. J. Mass Spectrom. 200 (2000) 71.
[16] I. Rogner, P. Birkett, E.E.B. Campbell, Int. J. Mass Spectrom. Ion Processes 156 (1996) 103.
[17] L. Zhou, A.A. Tuinman, R.N. Compton, A.S. Lahamer, Electrochem. Soc. Proc. 98 (1998) 493.
[18] D.M. Guldi, Y. Tian, J.H. Fendler, H. Hungerbühler, K.-D. Asmus, J. Phys. Chem. 99 (1995) 17673.
[19] M.P. Barrow, T. Drewello, Int. J. Mass Spectrom. 203 (2000) 111.
[20] N.L. Clipston, T. Brown, Y.V. Vasil'ev, M.P. Barrow, R. Herzschuh, U. Reuther, A. Hirsch, T. Drewello, J. Phys. Chem. A 104 (2000) 9171.
[21] Y.V. Vasil'ev, R.R. Absalimov, S.K. Nasibullaev, A.S. Lobach, T. Drewello, J. Phys. Chem. A 105 (2001) 661.
[22] B. Spengler, D. Kirsch, R. Kaufmann, Rapid Commun. Mass Spectrom. 5 (1991) 198.
[23] S. Lebedkin, S. Ballenweg, J. Gross, R. Taylor, W. Krätschmer, Tetrahedron Lett. 36 (1995) 4971.
[24] S.G. Penn, D.A. Costa, A.L. Balch, C.B. Lebrilla, Int. J. Mass Spectrom. Ion Processes 169 (1997) 371.
[25] M.P. Barrow, N.J. Tower, R. Taylor, T. Drewello, Chem. Phys. Lett. 293 (1998) 302.
[26] R. Taylor, M.P. Barrow, T. Drewello, J. Chem. Soc., Chem. Commun. (1998) 2497.
[27] M.S. Al-Jafari, M.P. Barrow, R. Taylor, T. Drewello, Int. J. Mass Spectrom. 184 (1999) L1.
[28] H. Nonami, S. Fukui, R. Erra-Balsells, J. Mass Spectrom. 32 (1997) 287.
[29] H. Nonami, K. Tanaka, Y. Fukuyama, R. Erra-Balsells, Rapid Commun. Mass Spectrom. 12 (1998) 285.
[30] B. Gigante, C. Santos, T. Fonseca, M.J.M. Curto, H. Luftmann, K. Bergander, M.N. Berberan-Santos, Tetrahedron 55 (1999) 6175.
[31] C. Siedschlag, H. Luftmann, C. Wolff, J. Mattay, Tetrahedron 55 (1999) 7805.
[32] L. Ulmer, J. Mattay, H.G. Torres-Garcia, H. Luftmann, Eur. J. Mass Spectrom. 6 (2000) 49.
[33] Y.Y. Vasil'ev, D. Wallis, M. Nüchter, B. Ondruschka, A.S. Lobach, T. Drewello, Chem. Commun. (2000) 1233.
[34] R. Zhang, K.J. Fisher, D.R. Smith, G.D. Willett, J.B. Peel, L. Gan, Y. Shi, Z. Gao, Eur. J. Mass Spectrom. 6 (2000) 161.
[35] L.M. Roth, Y. Huang, J.T. Schwedler, C.J. Cassady, D. Ben-Amotz, B. Kahr, B.S. Freiser, J. Am. Chem. Soc. 113 (1991) 6298.
[36] Y. Huang, B.S. Freiser, J. Am. Chem. Soc. 113 (1991) 9418.
[37] P.M. Lloyd, K.G. Suddaby, J.E. Varney, E. Scrivener, P.J. Derrick, D.M. Haddleton, Eur. Mass Spectrom. 1 (1995) 293.
[38] M.J. Deery, K.R. Jennings, C.B. Jasieczek, D.M. Haddleton, A.T. Jackson, H.T. Yates, J.H. Scrivens, Rapid Commun. Mass Spectrom. 11 (1997) 57.
[39] I.A. Mowat, R.J. Donovan, R.R.J. Maier, Rapid Commun. Mass Spectrom. 11 (1997) 89.